The Desorption Kinetics of Flat-Lying Benzene from Palladium (111)

M. Noel Rocklein,[†,§] Tyrone V. Arnold,[‡,||] Christopher M. Gerth,[⊥] and Donald P. Land*

Department of Chemistry, University of California, Davis, California 95616

Received: July 14, 2003; In Final Form: October 1, 2003

Benzene desorption from palladium (111) is investigated at low coverages (**$\theta \cong 0.026$** and 0.050, where θ is the fractional coverage of benzene molecules to palladium surface atoms). Desorption occurs at rates that can be readily monitored using laser-induced thermal desorption with Fourier transform mass spectrometry between 430 and 490 K. Other researchers have concluded that, at these coverages, all benzene is flat-lying, i.e., adsorbed with the molecular plane nearly parallel to the surface. The desorption kinetics are adequately described by a first-order rate law and the Arrhenius plots are linear. The data indicate that competitive decomposition reactions are not significant at these temperatures and coverages. The activation energy (E_a) and the preexponential factor (A) are determined at two different coverages and no coverage dependence is observed. At the 95% confidence level ($N = 9$ and 6, respectively), the kinetic parameters are $E_d = 169 \pm 9$ kJ/mol and $\log A_d = 17.3 \pm 1.1$ s^{-1} for $\theta \cong 0.05$, and $E_d = 170 \pm 7$ kJ/mol and $\log A_d = 16.9 \pm 0.8$ s^{-1} for $\theta \cong 0.026$. The high values for the preexponential factors indicate a significant gain in entropy between the adsorbed state and the transition state for desorption.

Introduction

Benzene is the prototypical aromatic molecule and has been the subject of numerous surface chemical and structural studies. Interest in the interactions of benzene with the palladium (111) surface arose due to the observation that this surface can catalyze the production of benzene from acetylene.[1] Also, reversible hydrogenation of unsaturated hydrocarbons, such as benzene,[2] over Group VIII metal catalysts, such as Pd,[3] is relevant for the storage of hydrogen for on-demand use in stationary or mobile fuel cells or for heat/combustion-based systems.[4−7] Tysoe et al.[8] studied the behavior of benzene on Pd(111) using thermal desorption spectroscopy (TDS) and also kinetic simulation. Several benzene desorption peaks were observed and attributed to different overlayer structures and adsorption geometries. The low coverage, high-temperature desorption peak was assigned to flat-lying benzene with higher coverages leading to increased crowding and a decrease in the benzene desorption temperature. It was also hypothesized that at the highest coverages the lowest temperature desorption peak was due to benzene adsorbed in a tilted or edge-on geometry. Spectroscopic evidence (including electron diffraction) for flat-lying benzene has been reported on several metals: on Pt(111) and Cu(110) surfaces,[9] on Ru(001),[10] on Ni(110),[11] on Rh(111),[12,13] and on a Ag film.[14] In addition to the geometry, the energetics and kinetics of the interaction of benzene with surfaces is important to know if one wishes to accurately model such interactions, particularly if one wishes to predict product ratios for surface reactions. However, it is difficult to obtain accurate measurements of such quantities with most surface analysis techniques.

In this report, we study the desorption kinetics of benzene from palladium (111) at low coverages using LITD-FTMS. One of the major advantages of using laser-induced thermal desorption Fourier transform mass spectrometry (LITD-FTMS) to obtain kinetic information for surface processes is the ability to simultaneously calculate both the activation energy (E_a) and the preexponential factor (Arrhenius constant, A).[15] Thus, no assumption needs to be made about the preexponential factor in order to calculate the energy barrier for a given reaction. In fact, the changes in the kinetics of surface reactions can be a sensitive probe for changes in the surface composition[16,17] and reveal details of adsorption behavior.[18] Similarly, such surface kinetics studies can aid in the interpretation of reaction mechanisms,[15−19] particularly if one employs isotopic labeling[19] or coverage dependent studies.[16,19] In particular, for systems where desorption is the predominant process, the ability to accurately measure both the activation barrier and preexponential factor allows one to draw inferences on the adsorption state, as well as the desorption process.[20] For some systems, desorption can be accurately modeled as a simple first-order process, as is observed here.

Experimental Methods

The palladium sample was originally cut from a boule purchased from Princeton Scientific. The wafer was oriented using Laue X-ray diffraction, ground and polished using diamond grit paper, diamond paste, and then alumina paste (ultimately down to 0.05 μm). All experiments are performed in an ultrahigh vacuum, surface analysis instrument (base pressure $< 3 \times 10^{-10}$ Torr) that has been described elsewhere.[21] The palladium sample (10−12 mm diameter, 1−2 mm thick) is suspended by tantalum wires, which have been spot-welded to the sides of the crystal and attached to the copper arms of a liquid nitrogen-cooled copper block. The wires provide resistive heating and conductive cooling. Surface temperatures are estimated with a type K thermocouple spot-welded to the back center of the sample. For cleaning, the surface is sputtered using 500 eV Ar^+ and then heated to above 1150 K for over 30 min. The annealing step minimizes sputter damage and allows impurities in the subsurface region to diffuse to the surface. This includes embedded argon, which may be observed during

* Author to whom correspondence should be addressed. E-mail: dpland@ucdavis.edu.
† Department of Chemistry, University of Colorado, Boulder, CO 80309.
‡ 3-M Corporation, San Ramon, CA 94583.
§ E-mail address: mnrocklein@yahoo.com.
|| E-mail address: tvarnold@mmm.com.
⊥ E-mail address: prokovief@aol.com.

10.1021/jp036038q CCC: $27.50
Published on Web 12/18/2003

LITD if not properly annealed. Sputter/anneal cycles are repeated until no impurities are detected by Auger electron spectroscopy. Low-energy electron diffraction (LEED) verifies Pd(111) surface order. To remove carbon, the sample is heated to 800 K in 5×10^{-6} Torr of oxygen until only O_2 desorbs during thermal desorption spectroscopy (TDS) after dosing a 300 K sample with > 4 L of oxygen. The presence of CO in the TDS would indicate that further reaction in oxygen is necessary.

Spectra-grade benzene (Fisher Chemical) was transferred to a glass ampule, and several freeze−pump−thaw cycles are performed to remove noncondensable gases using a secondary vacuum line with a base pressure in the 10^{-5} Torr range. Final purity is verified by FTMS under sensitive conditions (typically 100 scans, 64 K data points, at 7×10^{-9} Torr) and by comparison to published spectra.[22] For the higher coverage experiments, the surface is exposed to 0.33 L of benzene (L = Langmuir = 10^{-6} Torr·s) at 80 K using a doser-tube. All exposures are corrected for the ion gauge sensitivity factor for benzene of 5.7.[23] Calibration of the doser-tube exposures to ambient (backfill) exposures is accomplished by comparing the adsorbed quantity of benzene on the clean surface at 80 K as a function of exposure by each method. For a given exposure, the adsorbed quantity is estimated using the average ion intensity of *m*/*z* 78 ($C_6H_6^+$) obtained using LITD-FTMS over the entire surface (over 40 spots). The ratio of the initial slopes for the two uptake curves determines the enhancement factor provided by the doser-tube. For the lower coverage experiments, the surface is exposed to 0.18 L of benzene at 200 K, this time achieved via backfill (e.g., 1.0×10^{-8} Torr for 100 s divided by 5.7 to account for ion gauge sensitivity). Since the exposure is a product of time and pressure, the reproducibility is determined by the ability to measure these quantities. The accuracy of ion gauge pressure measurements is significantly worse than 10%, unless calibrated in situ. The gauge employed for these studies was only roughly calibrated against mass spectrometer signals, so the accuracy of the exposures is estimated to be only about 20%. However, the reproducibility of the ion gauge is estimated to be about 10%, while the ability to measure the time is significantly better than that. Therefore, the overall uncertainty in the reproducibility of the exposure is about 10%. Throughout this report, the 0.33 and 0.18 L exposures are referred to as $\theta \cong 0.05$ and $\theta \cong 0.026$ fractional coverages, respectively. These coverages are approximated using the uptake curves presented by Tysoe et al., which plot exposure against coverage.[8]

For the LITD-FTMS kinetic experiments, the sample is positioned in front of the FTMS cell after cleaning, cooling, and exposure to benzene. A Nd:YAG laser beam (1064 nm, 5 ns pulse width, ~ 20 mJ/pulse) is aligned through the FTMS cell and focused to produce a 1 mm diameter spot on the center of the sample. This yields a power density of $\sim 10^9$ W/cm^2, roughly 80% of the Pd-ablation threshold. Under these conditions, LITD-FTMS yields are typically independent of small variations in the laser output.[24] The entire sample is then quickly heated to the desired temperature and, upon temperature stabilization, LITD-FTMS is immediately initiated. A computer-controlled movable mirror repositions the laser in an outward spiral to allow sampling of over 40 independent (nonoverlapping) spots. A complete mass spectrum (*m*/*z* 10−120) is obtained for each position, at a rate of up to 1 Hz. The electron ionization parameters (10 ms electron beam width, <30 μA current) are sufficiently low so that an observable signal is only expected at these temperatures and coverages if the laser desorbs a burst of material from the surface. The low flux of material slowly desorbing via conventional thermal desorption is not sufficient to register a signal, thus allowing one to discriminate between conventional and laser-induced thermal desorption products. This is confirmed by periodically blocking the laser beam to observe that the background produces no observable mass peaks.

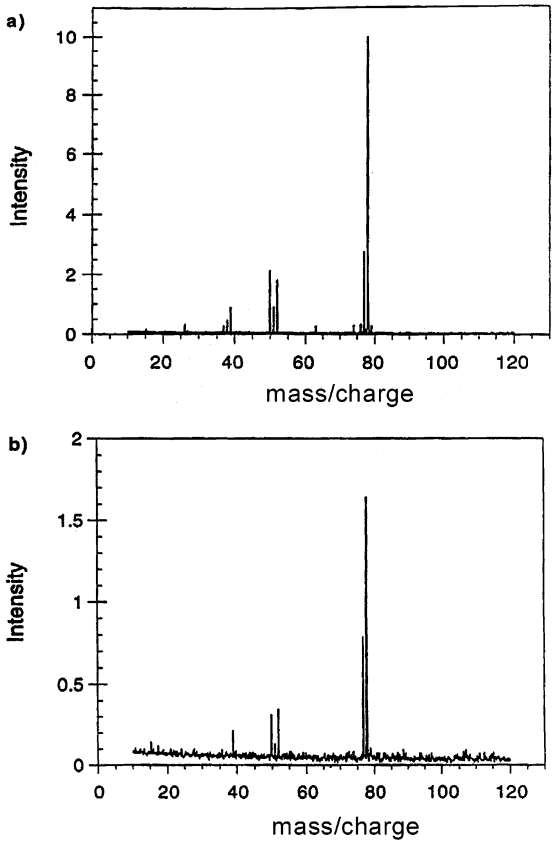

Figure 1. LITD/FTMS of benzene on Pd(111) at 458 K for an initial coverage of $\theta \cong 0.05$. The following two spectra are shown: (a) a mass spectrum from near the beginning of the kinetic acquisition. (b); a mass spectrum taken two minutes after the initial acquisition (note that the *y*-axis is expanded in Figure 1b).

Results

Figure 1a shows a mass spectrum using LITD-FTMS at 458 K for an initial benzene coverage of $\theta \cong 0.05$ near the beginning of the kinetic acquisition. Two minutes later, the benzene desorption yield (*m*/*z* 78) has decreased by a factor of 6, as shown in Figure 1b. Isothermal kinetic studies were also conducted for this initial coverage at 487, 482, 476, 470, 456, 447, 446, 437, and 429 K.

Figure 2 shows the decrease in *m*/*z* 78 intensity as a function of time at 458 K (circles). These are plotted on the same time axis as a similar experiment conducted at 446 K (squares). The displayed curves represent the best-fit according to eq 2 (see below). To obtain the rate constant (k) at each temperature, the data (intensity vs time, or I_i vs t_i) for each decay curve were fit to several different models, as shown below:

$$I_i = m_1 e^{-k^* t_i} \text{ (first-order decay)} \quad (1)$$

$$I_i = m_1 e^{-k^* t_i} + m_2 \text{ (first-order decay + intensity offset)} \quad (2)$$

$$I_i = m_1 e^{-k^* t_i} + m_2 e^{-k'^* t_i} \text{ (sum of two first-order decays)} \quad (3)$$

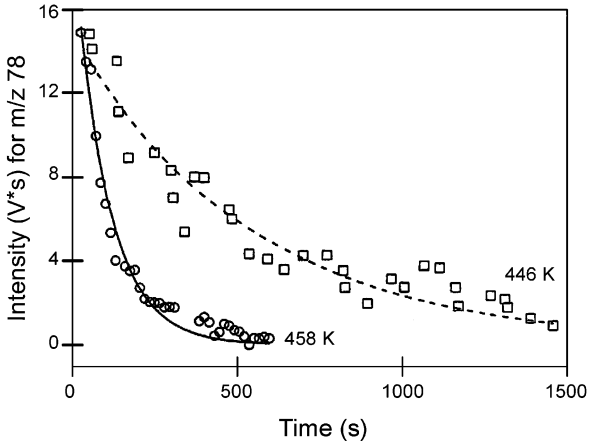

Figure 2. Benzene depletion on the Pd(111) surface as measured by LITD/FTMS for an initial coverage of $\theta \cong 0.05$. The *m*/*z* 78 signal is followed at 446 K (squares) and 458 K (circles).

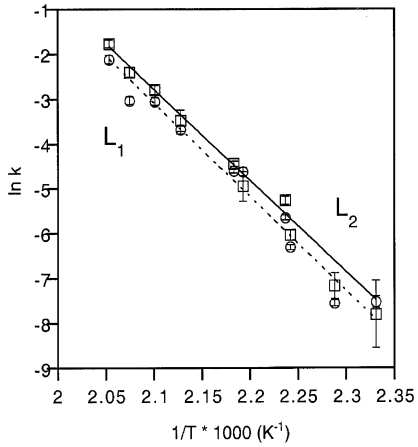

Figure 3. Plot of ln k_T vs $1/T$ to determine the activation energy and preexponential factor for an initial surface coverage of $\theta \cong 0.05$. Line L1 (circles) and line L2 (squares) arise from k_T values obtained using eqs 1 and 2, respectively. The vertical bars represent two standard errors ($\pm\sigma_T$) for each ln k_T value. The fits are weighted according to $1/\sigma_T^2$ (see text).

where k, k', m_1, m_2, and m_3 are adjustable parameters. Equation 1, representing a first-order decay, provides a reasonably good fit to most of the decay curves. However, for some of the higher-temperature experiments, the signals did not approach the baseline as quickly as might be expected. Equation 2 includes an empirical offset that may have some physical meaning if there were a relatively constant benzene background, some benzene readsorption, or some nonreacting and nondesorbing benzene adsorbed strongly to defect sites, etc. Equation 3 includes an additional exponential decay, which may arise from a secondary depletion effect such as reaction, slow thermal desorption, or slow evacuation from the chamber, etc. According to the *F*-test using χ^2 values, eq 2 provides a better fit than eq 1 for a majority of the kinetic experiments. According to the *F*-test, eq 3 was statistically better than eq 2 only at the two highest temperatures.

Figure 3 shows an Arrhenius plot (ln(k_T) vs $1/T$) for k values obtained at each temperature by using eq 1 (circles) or eq 2 (squares). The error bars indicate $\pm\sigma_T$, the standard error in ln(k_T) (obtained by $\sigma_T = \sigma_k/k$). Weighted linear regression of each data set produces line L_1 and line L_2, respectively (each data point is weighted according to $1/\sigma_T^2$). The slope is equal to $-E_a/R$ and the *y*-intercept is equal to ln(A), where E_a is the apparent activation energy, R is the gas constant (J mol^{-1} K^{-1}),

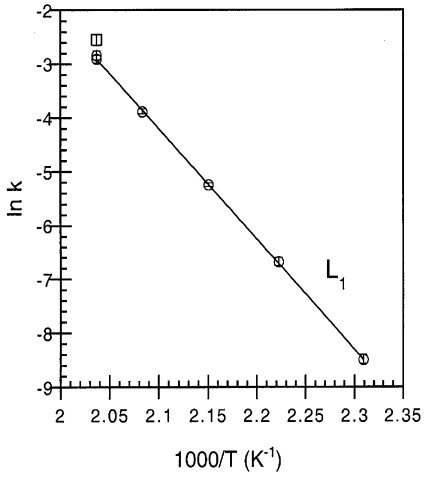

Figure 4. Plot of ln k_T vs $1/T$ to determine the activation energy and preexponential factor for the initial initial surface coverage of $\theta \cong 0.05$. The circles and L1 arise from k_T values obtained by using eq 1. The square represents a k_T value calculated for a single temperature, 491 K, using eq 2; this value was not used in the overall analysis. The vertical bars represent two standard errors ($\pm\sigma_T$) for each ln k_T value. The fit is weighted according to $1/\sigma_T^2$ (see text).

and A is the preexponential factor (s^{-1}). At the 95% confidence level ($N = 9$), line L_1 yeilds $E_a = 174 \pm 6$ kJ/mol and $A = 10^{17.7\pm0.7}$ s^{-1}. From L_2, $E_a = 169 \pm 9$ kJ/mol and $A = 10^{17.3\pm1.1}$ s^{-1}. These kinetic parameters obtained by the two methods are indistinguishable at the 95% confidence level. Line L_2, however, has a lower χ^2 value (by a factor of 6).

Depletion effects due to the actual LITD measurements can be ignored for this system. On the basis of the macroscopic Pd surface area and the laser spot size, the maximum amount of benzene removed from any laser shot is only about 1% of the instantaneous surface concentration. Under the assumption that the adsorbate is infinitely mobile at these temperatures and will disperse to replace the benzene removed from the previous laser shot, the observed depletion kinetics are not significantly affected. This is tested by recalculating the rate constant at each temperature using corrected surface concentrations (actually, LITD-FTMS *m*/*z* 78 signal intensities). Each surface concentration is corrected by adding 1% of the intensity obtained at *all* previous laser spots (each amount decreased exponentially with time using approximate k values obtained previously). The kinetic parameters (E_a and log A) were modified by less than 3%.

Benzene depletion kinetics are also investigated at approximately half the initial coverage ($\theta \cong 0.026$). Decay curves were observed for *m*/*z* 78 at 491, 479, 463, 447, and 433 K, and again at 491 K. In all cases, except for one of the 491 K experiments, the signal decayed appropriately to the baseline according to first-order desorption kinetics. Further, natural log plots versus time were linear, suggesting a single-exponential decay model. Figure 4 shows the ln(k_T) values (circles) plotted as a function of reciprocal temperature. Equation 1 is used to obtain all k values since eq 2 provided a better fit for only one of the 491 K experiments, according to the *F*-test. This additional value is displayed in Figure 4 (as a square); however, it was not used in the analysis. The error bars represent the standard errors ($\pm\sigma_T$) in each ln(k_T) value. Weighted linear regression ($1/\sigma_T^2$) is performed and the coefficients yield the kinetic parameters: $E_a = 170 \pm 7$ kJ/mol and $A = 10^{16.9\pm0.8}$ s^{-1} at the 95% confidence level ($N = 6$). These are similar to those reported above.

Discussion

Tysoe et al. [8] observe three benzene desorption peaks using thermal desorption spectroscopy at 8 K/s for benzene adsorbed onto Pd(111) at 200 K. The peaks fill sequentially with increasing exposure and are identified as γ (centered at 520 K), β (380 K), and α (280 K). Structural models are proposed to explain the behaviors, as summarized. For $\theta < 0.05$, flat-lying benzene exists on the surface with no nearest neighbors. Decomposition occurs as evidenced by hydrogen evolution near 560 K and negligible benzene desorption. The γ state corresponds to $\theta = 0.05$ to 0.09, where each adsorbed benzene molecule has up to 3 near neighbor interactions. The β state corresponds to $\theta = 0.09$ to 0.14, where each flat-lying benzene molecule has from 3 to 6 near neighbor interactions. The α state corresponds to $\theta = 0.14$ to 0.21, where benzene adsorption into the densely packed first layer is activated and requires molecular reorientation (tilting) to accommodate such high coverages. Finally, using simple first-order analysis and a preexponential factor of 10^{13} s^{-1}, the authors estimate a desorption barrier of 130 kJ/mol for γ, and 95 kJ/mol for β.

The benzene depletion data in this report indicate that a coverage dependence is not observed below $\theta \cong 0.05$. This may be expected for these coverages given that there are no near-neighbor interactions; any repulsive interactions should affect either the desorption kinetics or the branching ratios for decomposition versus desorption. On the basis of the similarity in results for the two coverages, and based on the individual decay curves analyzed by either eqs 1, 2, or 3, it appears that there is only one dominant mechanism that controls the depleting benzene signal in LITD/FTMS as a function of time, for these coverages in the temperature regime of 430 to 490 K. This is also supported by the linearity of the Arrhenius plots.

A typical value cited for the preexponential term for desorption is 10^{13} s^{-1}. This is calculated using transition state theory for a species with no internal modes trying to escape from a one-dimensional potential well. The large value of 10^{17} s^{-1} observed here indicates that there is a large gain in entropy in going to the transition state. This generally implies that many more dynamical modes are active in the transition state, such as translation or rotation, as may be the case for benzene desorption. Decomposition, on the other hand, typically produces a lower preexponential value than does desorption for adsorbed molecules, by 1 to 3 orders of magnitude.[25] Campbell et al. compare the dehydrogenation rates for various hydrocarbons on metal surfaces and present an average preexponential factor of 10^{11} s^{-1}. The low value of the preexponential is attributed to the fact that dynamical motions such as rotations, which make large contributions to the entropy, are converted to vibrations which contribute negligibly to the transition state partition function. It is therefore unlikely that benzene decomposition (involving the formation of a palladium−hydrogen bond) would produce such a high preexponential factor. In fact, the catalytic activity of Pd with respect to dehydrogenation most likely results from the stabilization of the transition state by formation of a metal-hydride bond. Given our large preexponential value and the kinetic behavior previously presented, thermal desorption is likely the sole or dominant mechanism for the decreasing surface concentrations of benzene, as observed in these experiments.

It should be noted that the data observed here are not in fundamental conflict with Tysoe's assertion that benzene decomposition dominates below $\theta = 0.05$. Their results arise from TDS at 8 K/s where a significant portion decomposes. Benzene decomposition also dominates desorption for small coverages on Pd(111) during TDS at 1 K/s, as evidenced by H_2 desorption near 560 K, and near 540 K at higher coverages.[26] Hydrogen (H_2) should evolve from the surface concurrent with and/or slightly after benzene decomposition since hydrogen adatoms readily recombine and desorb between 270 and 400 K on the clean surface.[27,28] We also observe both desorption and decomposition during TDS at 3 K/s, even for $\theta \cong 0.026$. A small amount of benzene desorption is observed between 440 and 530 K (centered near 475 K). In a separate FTMS-TDS experiment (using a lower magnetic field strength to accommodate the limitations imposed by our analog-to-digital converter at 2 MHz), H_2 desorption is also observed between 540 and 640 K (centered at 585 K), indicating decomposition. Prior to the LITD-FTMS experiments, benzene desorption/detection was initially unexpected for this low coverage; however it may arise from the high sensitivity of our FTMS or from a low number of surface-defect sites. The fact that we observe any benzene desorption during TDS (and at lower temperatures than H_2 desorption), supports our conclusion that with LITD-FTMS we are monitoring desorption and not decomposition, given only one dominant mechanism. Most importantly, during the *isothermal* LITD studies, the benzene depletion occurs on a much longer time scale and at lower temperatures where the dominant mechanism for benzene removal appears to be desorption.

Conclusions

The desorption kinetics for flat-lying benzene on Pd(111) have been observed using LITD-FTMS, and kinetic parameters for desorption have been measured. For low coverages ($\theta \cong 0.026$, with presumably negligible benzene repulsion), the best values are $E_d = 170 \pm 7$ kJ/mol and $A_d = 10^{16.9\pm0.8}$ s^{-1} (95% confidence, $N = 6$). First-order kinetics using a single exponential decay appropriately describe the desorption process from 430 K to about 490 K. At approximately twice the coverage (($\theta \cong 0.05$), $E_d = 169 \pm 9$ kJ/mol and $A_d = 10^{17.3\pm1.1}$ s^{-1}. It is concluded that above these temperatures competitive decomposition reactions become relevant, but that desorption predominates in these studies. The relatively high values for the preexponential factor are significantly different than the 10^{13} s^{-1} typically assumed using rudimentary transition state theory, and lead to a correspondingly higher value for the activation barrier, as well. The ability to accurately determine both parameters should be of great utility for models, particularly those that attempt to extrapolate to conditions outside of those normally encountered in standard surface science techniques.

Acknowledgment. Some of the data have been previously presented in the Masters theses of authors T.V.A. (1995) and author C.M.G.(1997), respectively, from the University of California, Davis. We acknowledge National Science Foundation Grant CHE-0111275 for partial funding of this work.

References and Notes

(1) Lambert, R. M.; Ormerod, R. M. *Springer Ser. Surf. Sci.* **1994**, *34*, 89.

(2) Startsev, A. N.; Aleshina, G. I.; Aksenov, D. G.; Rodin, V. N. *Kinet. Catal.* **1998**, *39*, 363.

(3) Vasquez, N., Jr.; Madix, R. J. *J. Catal.* **1998**, *178*, 234.

(4) Chen, J.; Wu, F.; Zhu, Y. *Taiyangneng Xuebao* **1998**, *19*, 360.

(5) Chen, J.; Lu, S.; Zhu, Y. *Ranliao Huaxue Xuebao* **1998**, *26*, 543.

(6) Newson, E.; Uenala, E.; Geissler, K.; Hottinger, P.; Truong, T. B.; Von Roth, F. *Hydrogen Energy Progress XII, Proceedings of the World Hydrogen Energy Conference, 12th, Buenos Aires, June 21−26, 1998* **1998**, *2*, 953.

(7) Taube, M.; Rippin, D.; Knecht, W.; Hakimifard, D.; Milisavijevic, B.; Gruenenfelder, N. *Int. J. Hydrogen Energy* **1985**, *10*, 595.

(8) Tysoe, W. T.; Ormerod, R. M.; Lambert, R. M.; Zgrablich, G.; Ramirez-Cuesta, A. *J. Phys. Chem.* **1993**, *97*, 3365.

(9) Haq, S.; King, D. A. *J. Phys. Chem.* **1996**, *100*, 16957.
(10) Jakob, P.; Menzel, D. *J. Chem. Phys.* **1996**, *105*, 3838.
(11) Huber, W.; Weinelt, M.; Zebisch, P.; Steinrueck, H. P. *Surf. Sci.* **1991**, *253*, 72.
(12) Lin, R. F.; Blackman, G. S.; Van Hove, M. A.; Somorjai, G. A. *Acta Crystallogr., Sect. B: Struct. Sci.* **1987**, *B43*, 368.
(13) Van Hove, M. A.; Lin, R. F.; Somorjai, G. A. *J. Am. Chem. Soc.* **1986**, *108*, 2532.
(14) Moskovits, M.; DiLella, D. P. *J. Chem. Phys.* **1980**, *73*, 6068.
(15) Abdelrehim, I. M.; Thornburg, N. A.; Sloan, J. T.; Caldwell, T. E.; Land, D. P. *J. Am. Chem. Soc.* **1995**, *117*, 9509.
(16) Abdelrehim, I. M.; Caldwell, T. E.; Land, D. P. *J. Phys. Chem.* **1996**, *100*, 10265.
(17) Caldwell, T. E.; Abdelrehim, I. M.; Land, D. P. *Langmuir* **1998**, *14*, 1407.
(18) Caldwell, T. E.; Abdelrehim, I. M.; Land, D. P. *J. Phys. Chem. B* **1998**, *102*, 562.
(19) Caldwell, T. E.; Land, D. P. *J. Phys. Chem. B* **1999**, *103*, 7869.
(20) Thornburg, N. A.; Abdelrehim, I. M.; Land, D. P. *J. Phys. Chem. B* **1999**, *103*, 8894.
(21) Abdelrehim, I. M.; Thornburg, N. A.; Land, D. P. *Rev. Sci. Instrum.* **1997**, *68*, 4572.
(22) McLafferty, F. W. *The Wiley/NBS registry of mass spectral data*; Wiley: New York, 1989.
(23) Otvos, J. W.; Stevenson, D. P. *J. Am. Chem. Soc.* **1956**, *78*, 546.
(24) Land, D. P.; Abdelrehim, I. M.; Thornburg, N. A.; Sloan, J. T. *Anal. Chim. Acta* **1995**, *307*, 321.
(25) Campbell, C. T.; Sun, Y. K.; Weinberg, W. H. *Chem. Phys. Lett.* **1991**, *179*, 53.
(26) Waddill, G. D.; Kesmodel, L. L. *Phys. Rev. B: Condens. Matter* **1985**, *31*, 4940.
(27) Gdowski, G. E. F.; Madey, T. E.; Stulen, R. H. *Surf. Sci.* **1987**, *181*, L147.
(28) Guo, X. H., A.; Yates, J. T., Jr. *Surf. Sci.* **1988**, *203*, L672.